

Durability of mechanically loaded engineered cementitious composites under highly alkaline environments

Mustafa Şahmaran^a, Victor C. Li^{b,*}

^a Department of Civil Engineering, Gaziantep University, 27310 Gaziantep, Turkey

^b Department of Civil and Environmental Engineering, The University of Michigan, Ann Arbor, MI 48109, United States

Received 19 March 2007; received in revised form 10 September 2007; accepted 10 September 2007

Available online 25 September 2007

Abstract

Durability of mechanically loaded Engineered Cementitious Composites (ECC) is investigated in this paper. ECC offers significant potential for durable civil infrastructures, due to its high tensile strain capacity of more than 3%, and controlled micro-crack width of less than 80 µm. An experimental study was designed to investigate the durability of ECC material with regard to cracking and healing under combined mechanical loading and environmental loading conditions. ECC coupon specimens were firstly pre-loaded under uniaxial tension to different strain levels, and then exposed to an alkaline environment up to 3 months at 38 °C and reloaded up to failure. The reloaded specimens showed slight loss of ductility and tensile strength, but retained the multiple micro-cracking behavior and tensile strain capacity of more than 2% (about more than 200 times that of normal concrete and normal fiber reinforced concrete). The test results indicated strong evidence of self-healing of the micro-cracked ECC material, which can still carry considerable tensile stress and strain and restore nearly the original stiffness. The phenomenon of self-healing effectively closes the micro-cracks even after one month exposure period. In addition to coupon specimens, ECC bar specimens were also immersed in alkali solution at 80 °C in accordance to ASTM C 1260 to determine their length change due to alkali silica reaction (ASR). The ECC bar specimens did not show any expansion at the end of 30 days soaking period. Therefore, these test results indicated that ECC, both virgin and micro-cracked, remain durable despite exposure to a high alkaline environment. The risk of ASR in ECC is determined to be low.

© 2007 Elsevier Ltd. All rights reserved.

Keywords: Engineered Cementitious Composites (ECC); Cracking; Alkaline environment; ASR; Self-healing

1. Introduction

Recently, many cementitious composite materials have been developed for potential civil engineering applications. Amongst these, Engineered Cementitious Composite (ECC) represents a unique type of high performance fiber reinforced cementitious composite (HPFRCC) which features high tensile ductility with moderate fiber volume fraction, typically 2% by volume [1]. The mixture design of current ECC contains controlled quantities and types of cement, sand, fly ash, water, chemical admixtures, and short, randomly oriented polyvinyl alcohol (PVA) fiber.

ECC has been engineered to satisfy various field performance requirements such as high durability, or impact load resistance. Unlike ordinary concrete materials, ECC strain-hardens after first cracking, similar to a ductile metal, and demonstrates a strain capacity of 300–500 times greater than normal and fiber reinforced concrete. Even at large imposed deformation of several percent, crack widths of ECC remain small, less than 80 µm [2]. To accommodate large deformations, rather than forming a single crack that widens with increasing load as is typical in concrete or tension-softening fiber reinforced concrete (FRC), ECC forms numerous micro-cracks which allow the material to undergo large tensile inelastic straining. The tight crack width of ECC is important to the durability of ECC structures as the tensile ductility is to the structural safety. This

* Corresponding author. Tel.: +1 734 764 3368; fax: +1 734 764 4292.
E-mail address: vccli@umich.edu (V.C. Li).

high performance is made possible through the use of steady-state flat crack models that provide quantitative links between micro-mechanical properties such as fiber bridging properties and matrix toughness, and composite mechanical behavior such as steady-state cracking stress and maximum crack width.

High performance fiber reinforced cementitious composite (HPFRCC) usually refer to the class of fiber reinforced cementitious composites that show macroscopic pseudo strain hardening behavior under uniaxial tension [3]. HPFRCCs are usually achieved by introducing large volume fractions of fibers (typically above 5%) [4,5]. In ECC, however, only a moderate volume fraction of fibers (1–2%) is utilized to facilitate production in either a regular casting process or an extrusion process. In addition to its pseudo-strain hardening behavior and high strain capacity under tensile loads, ECC also has high ultimate tensile strength and modulus of rupture, high fracture toughness and isotropic properties [6]. This high performance of ECC is unique, even among HPFRCC materials, and can only be achieved when certain micro-mechanical conditions are met. Fracture toughness of matrix, fiber/matrix interface bond strength, and initial flaw size are some of the micro-mechanical parameters that govern the composite performance. These parameters may be sensitive to environmental exposure conditions [7]. Although a great deal of research has been directed towards addressing durability of PVA fiber under aggressive environment, little information is currently available on the long-term durability of cracked (mechanically loaded) and uncracked (virgin) composite (fiber plus matrix) under aggressive environments. One of the environments that could affect the microstructure and composite properties of ECC is a high alkaline environment. In addition to high alkaline matrix pore water solution, ECC can come into contact with alkaline media through interaction with a variety of alkaline chemicals, soil (or solutions diffusing through soil) and sea water.

In general, PVA fibers are considered to have a very good durability in alkaline environments, and test results have shown that PVA fiber mechanical properties are largely retained after accelerated exposures [8]. However, ECC structural members may be exposed to high alkaline environments and alkalis will penetrate through micro-cracks or even the uncracked matrix that could lead to modifications in the material microstructure and hence changes in the composite properties. Due to the delicate balance of cement matrix, fiber, and matrix/fiber interface properties, the strain capacity of ECC may change under high alkaline exposure conditions. Therefore, the durability of composites (fiber plus matrix – ECC) must first be evaluated before it can be used in real field conditions.

This paper gives the results of an investigation on the durability of mechanically pre-loaded ECC material under high alkaline environment. ECC coupon specimens were pre-loaded under uniaxial tension to the strain of 1.0% and 2.0%, to simulate different strain levels applied to an

in-service structure. The pre-applied strain can be a combination of strain due to vehicle load, prestressing load, shrinkage, thermal load, etc. Later on, the specimens were exposed to a high alkaline environment up to 3 months and then re-loaded up to failure. Direct tensile test was used to analyze the mechanical properties and durability of pre-loaded and virgin ECC exposed to high alkaline environment. The effect of autogenous healing was assessed by measuring the retained stiffness, ultimate tensile strength and tensile strain capacity of ECC. In addition to tensile specimens, ECC bar specimens were prepared and expansion of ECC bar specimens immersed in alkaline solution at an elevated temperature was evaluated according to ASTM C1260. These experimental results, taken together, provide useful information on the durability of ECC under high alkaline environment.

2. Design of Engineered Cementitious Composites

The first priority when designing ECC material is to ensure the formation of multiple cracks and strain-hardening behavior under load. This allows large deformations to be distributed over multiple micro-cracks. The basis of multiple micro-cracking and strain hardening within ECC is the propagation of steady-state cracks which were first characterized by Marshall and Cox [9], and extended to fiber reinforced cementitious composites by Li and Leung [10] and Lin et. al. [11]. By forming steady state “flat cracks” which maintain a constant crack width while propagating, rather than Griffith-type cracks which widen during propagation as in typical tension-softening fiber reinforced cementitious materials, ECC material exhibits multiple micro-cracks which saturate the specimen while undergoing strain-hardening during extreme tensile deformation. The formation of multiple steady-state cracking is governed by the bridging stress versus crack width opening relation along with the cracking toughness of the mortar matrix. To achieve this phenomenon the inequality shown in Eq. (1) must be satisfied,

$$J'_b = \sigma_0 \delta_0 - \int_0^{\delta_0} \sigma(\delta) d\delta \geq J_{tip} \approx \frac{K_m^2}{E_m} \quad (1)$$

where J'_b is the complimentary energy shown in Fig. 1, σ_0 and δ_0 are the maximum crack bridging stress and corresponding crack opening, J_{tip} is the fracture energy of the mortar matrix, K_m is the fracture toughness of the mortar matrix, and E_m is the elastic modulus of the mortar matrix. In addition to the fracture energy criterion, a strength criterion expressed in Eq. (2) must be satisfied,

$$\sigma_0 > \sigma_{fc} \quad (2)$$

where σ_0 is the maximum crack bridging stress and σ_{fc} is the first cracking strength of the mortar matrix. For saturated multiple cracking, Wang and Li [12] found that Eq. (2) must be satisfied at each potential crack plane, where σ_{fc} is understood as the cracking stress on that crack plane.

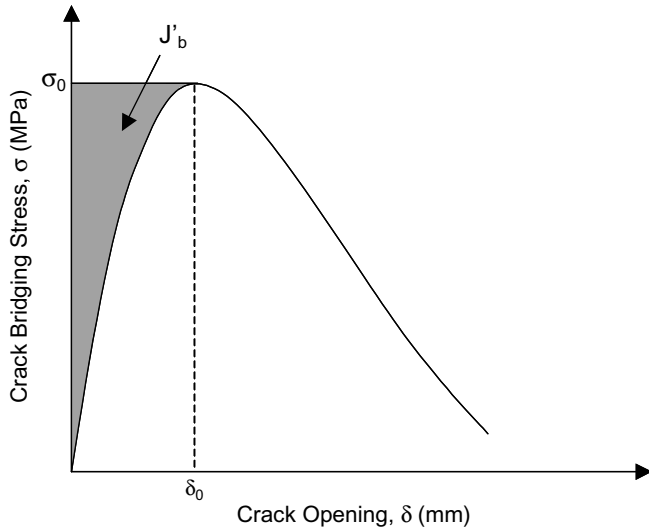


Fig. 1. Crack bridging stress versus crack opening relation.

Once an ECC mixture is selected which sufficiently meets the two above criteria, the formation of multiple steady-state cracks, and strain-hardening performance, can be realized. However, in addition to forming these cracks, the material must also be designed to exhibit crack widths below the 100 μm threshold limit. This can be achieved through tailoring of the crack bridging versus crack opening relation referenced in Eq. (1). The maximum steady-state crack width exhibited during ECC multiple cracking can be assumed to be δ_0 , the crack width corresponding to the maximum crack bridging stress, σ_0 , as shown in Fig. 1. If the crack width were to grow beyond δ_0 , the crack bridging stress would begin to fall, in which case the crack would localize and multiple crack formation would cease. By keeping δ_0 below the 100 μm threshold, the ECC material can exhibit multiple cracking while keeping a tight crack width necessary for durability consideration.

Lin et al. [11] proposed the formulation of the crack bridging stress versus opening relationship based on summing the bridging force contribution of fibers that cross a given crack plane. This relation is expressed in Eq. (3).

$$\sigma(\delta) = \frac{4V_f}{\pi d_f^2} \int_{\phi=0}^{\pi/2} \left(\int_{z=0}^{(L_f/2)\cos\phi} P(\delta)e^{f\phi} p(\phi)p(z)dz \right) d\phi \quad (3)$$

where V_f is the fiber volume fraction, d_f is the fiber diameter, ϕ is the orientation angle of the fiber, L_f is the fiber length, z is the centroidal distance of a fiber from the crack plane, f is a snubbing coefficient, and $p(\phi)$ and $p(z)$ are probability density functions of the fiber orientation angle and centroidal distance from the crack plane, respectively. $P(\delta)$ is the pullout load versus displacement relation of a

single fiber aligned normal to the crack plane, also described in Lin et al. [11]. Fiber/matrix interfacial properties are embedded in this $P(\delta)$ function. The factor $e^{f\phi}$ accounts for the changes in bridging force for fibers crossing at an inclined angle to the crack plane.

Using these basic micro-mechanical models to tailor the ECC material, a composite can be designed to undergo large deformations, up to several percent, without sacrificing low permeability due to large crack widths. The application of material design procedures, such as those outlined above, allow materials engineers to carefully match material characteristics to specific structural demands, such as strain capacity and low permeability.

3. Experimental studies

3.1. Materials, mixture proportions, and specimen preparation

The components of ECC material are similar to typical fiber reinforced cement composites, consisting of ordinary portland cement (C), Class-F fly ash (FA) with a lime content of 10.44%, silica sand with an average and maximum grain size of 110 μm and 200 μm , respectively, water, polyvinyl alcohol (PVA) fibers, and a high range water reducing admixture (HRWR). The PVA fibers are purposely manufactured with a tensile strength, elastic modulus, and maximum elongation matching those needed for strain-hardening performance [13]. Additionally, the surface of the PVA fibers is coated with a proprietary hydrophobic oiling agent 1.2% by weight to tailor the interfacial properties between fiber and matrix for strain-hardening performance. The mechanical and geometrical properties of the PVA fibers used in this study are shown in Table 1.

Standard ECC mixture (M45) was used in this investigation, details of which are given in Table 2. ECC mixture was prepared in a standard mortar mixer at water to cementitious material (W/CM) ratio of 0.27 and had a fly ash-cement ratio (FA/C) of 1.2 by mass. The compressive strength test results of standard ECC mixture at 7 and 28 days are also listed in Table 2. The compressive strength was computed as an average of three standard $\varnothing 75 \times 150$ -mm cylinder specimens.

To measure the expansion due to high alkaline environment, four ECC bar samples ($25 \times 25 \times 285$ mm) were cast and tested according to ASTM C1260. The ECC bars were demoulded after 24 h and cured in water at 80 $^\circ\text{C}$ for another 24 h. After initial reading of the lengths, the ECC bars were immersed in 1 N sodium hydroxide (NaOH) solution at 80 $^\circ\text{C}$. The expansion of the ECC bars was recorded up to 30 days.

Table 1
Mechanical and geometrical properties of PVA fiber

Nominal strength (MPa)	Apparent strength (MPa)	Diameter (μm)	Length (mm)	Young's modulus (GPa)	Elongation (%)
1620	1092	39	8	42.8	6.0

Table 2
Mixture properties of ECC and mortar

	ECC (M45)
FA/C	1.2
W/CM ^a	0.27
Water (W), kg/m ³	331
Cement (C), kg/m ³	570
Fly ash (FA), kg/m ³	684
Sand (S), kg/m ³	455
Fiber (PVA), kg/m ³	26
HRWR, kg/m ³	4.9
7-day compressive strength, MPa	38.1
28-day compressive strength, MPa	50.2

^a CM: Cementitious materials. (cement + fly ash).

To characterize the direct tensile behavior of the ECC mixture, $152.4 \times 76.2 \times 12.7$ mm coupon specimens were prepared. All specimens were demoulded at the age of 24 h, and moisture cured in plastic bag at $95 \pm 5\%$ RH, 23 ± 2 °C for 7 days. The specimens were then air cured in laboratory medium at $50 \pm 5\%$ RH, 23 ± 2 °C until the age of 28 days. The direct tensile cracks were introduced in the coupon specimens as described in the following section. After pre-cracking, these specimens were stored in sodium hydroxide solution at 38 °C for up to 90 days.

3.2. Uniaxial tensile test

After 28 days of curing, the coupon specimens were pre-cracked by straining to 1.0% and 2.0% in direct tensile strain to achieve various amounts of micro-cracks before placing in the 1 N sodium hydroxide solution at 38 °C. Before testing, aluminum plates were glued to both ends of the coupon specimen to facilitate gripping. Tests were conducted on an MTS machine with 25 kN capacity under displacement control at a rate of 0.005 mm/s. A typical stress–strain curve obtained when the specimens were

Table 3
Crack numbers and average crack widths of pre-cracked ECC coupons

Mix ID	Pre-loading tensile strain (%)	Average crack widths (µm)	Crack number
ECC	1.0	~44	12
(M45)	2.0	~55	21

mechanically pre-cracked at 28 days before exposure is shown in Fig. 2. When the tensile strain reached the required pre-determined strain value, the tensile load was released. A small amount of crack closure occurred on unloading. To account for this, all crack width measurements were conducted in the unloaded stage. The widths of the crack were measured on the surface of the specimens by an optical microscope. Table 3 shows the pre-loading tensile strain value, their corresponding average crack widths, and number of cracks within the pre-cracked coupon specimens. The gage length used in these measurements was about 50 mm. As seen from Table 3, even at large uniaxial tensile strain level (2.0%), crack widths of ECC remain nearly constant, while the number of cracks on tensile surface of the ECC specimens increased. As expected, a higher tensile strain coincides with more cracks.

Fig. 2 shows also the tensile properties of ECC specimens that had been pre-cracked to 1% or 2% strain levels, then unloaded, and immediately reloaded. Thus, these specimens had no time to undergo any crack healing which is found in specimens immersed to alkali solution as explained later. As expected, there is a remarkable difference in initial stiffness between virgin specimen and pre-cracked specimen under direct tension. This is due to re-opening of cracks within pre-cracked specimens during reloading [14]. The opening of these cracks offers very little resistance to load, as the crack simply opens to its previous crack width before fiber bridging is re-engaged. Once fiber bridging is re-engaged, however, the load capacity resumes,

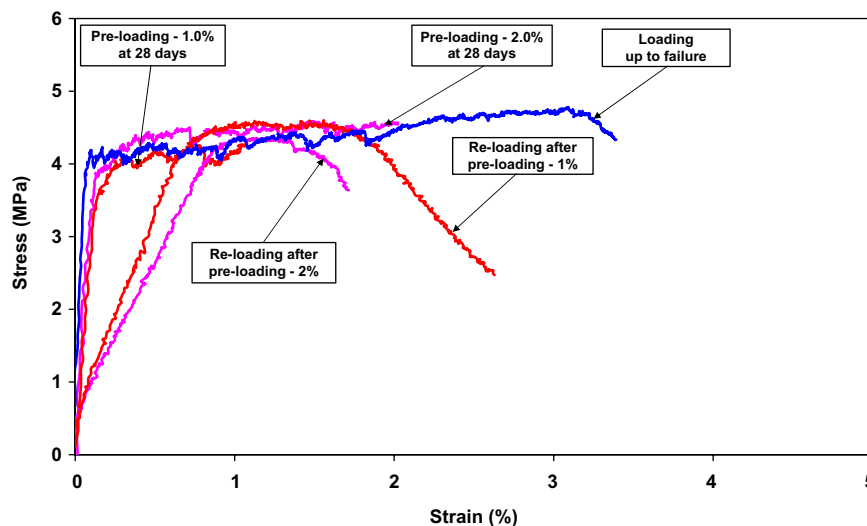


Fig. 2. A typical tensile stress–strain curves for pre-loading and re-loading ECC (M45) at 28 days.

and further tensile straining of the intact material can take place.

The pre-loaded ECC specimens were then continuously immersed in 1 N sodium hydroxide solution at 38 °C, together with some uncracked (virgin) specimens without pre-loading. The solution was made by adding 40 g of sodium hydroxide per liter of tap water. The alkali solution is replaced with a fresh solution at the end of each month. Reloading under direct tension of specimens having exposed to 30 and 90 days alkaline solution was conducted and their stress–strain curves were recorded. For control purpose, virgin specimens were also tested after 30 and 90 days additional curing in laboratory condition ($50 \pm 5\%$ RH, 23 ± 2 °C). The average tensile strain capacity, ultimate tensile strength and residual crack width of ECC were calculated from four specimens.

4. Results and discussion

4.1. Accelerated mortar bar test

The performance of ECC under high alkaline medium was tested according to ASTM C1260. ECC bars were immersed into an 80 °C, 1 N sodium hydroxide solution. The length change of the ECC bars was measured up to 30 days. Fig. 3 shows expansive behavior of the ECC. The classification ranges given from the ASTM C1260 are also illustrated graphically in Fig. 3 by horizontal grid-lines. The ECC bars showed no or negative expansion in the 30 days exposure period of sodium hydroxide solution at 80 °C, the negative expansion presumably due to autogenous shrinkage. Normally, moist curing is the best way to minimize autogenous shrinkage, but still, the shrinkage can occur within a concrete element, even when the exterior surfaces are exposed to 100% moist curing [15].

Therefore, ECC performed very well under high alkaline medium at an elevated temperature. One of the main rea-

sons of low expansion of ECC could be a result of non-reactive silica sand. The other reason of low expansion of ECC could be a result of high volume fly ash content. The addition of fly ash (especially Class-F fly ash) reduces the alkalinity of the pore solution due to the consumption of calcium hydroxide as a result of pozzolanic reaction [16]. The high amount of fly ash content is also expected to refine pore structure and then reducing alkali diffusion from the host solution into the sample and binding of alkalis into pozzolanic calcium silicate hydrates [16–18]. Moreover, the reduction in the alkali silica reaction expansion may be due to the use of micro-fibers (PVA fiber) in the production of ECC. The influence of micro-fiber addition on the alkali silica expansion has also been examined by other researchers [19–21], and according to their test results, it is plausible that micro-fibers aid in suppressing the expansion in the matrix induced by alkali silica reaction.

4.2. Uniaxial tensile behavior

Fig. 4 shows the tensile behavior of ECC mixtures cured in air at different ages, after an initial 7 days moist curing. These ECC composites exhibited a strain capacity of more than 3% at 28 days. The strain capacity measured after 28 days is slightly lower than the 7-day strain capacity (Fig. 4 and Table 4) for ECC (M45) mixture; however the observed 3.0% strain capacity remains acceptable for an ECC. The overall effect of this slight drop in long-term strain capacity is minimal. Based on the similarity of test results up to (28 + 90) days, the tensile strain capacity seems to stabilize at about 3.0% after 28 days. The time dependent strain capacity change described above has been known for sometime and is ascribed to the increase in fiber/matrix interface properties and matrix toughness associated with the continued cement hydration process [22].

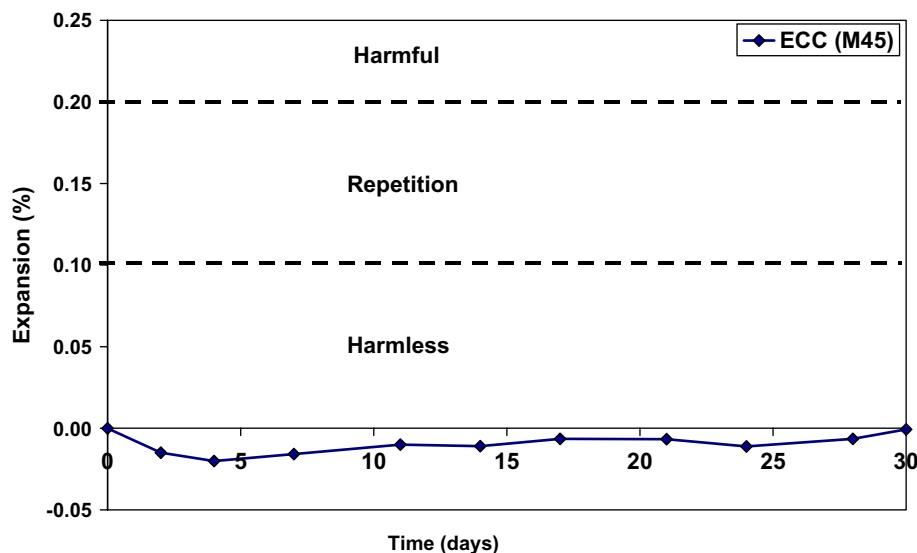


Fig. 3. Length change of ECC (M45) mixture (ASTM C1260-94).

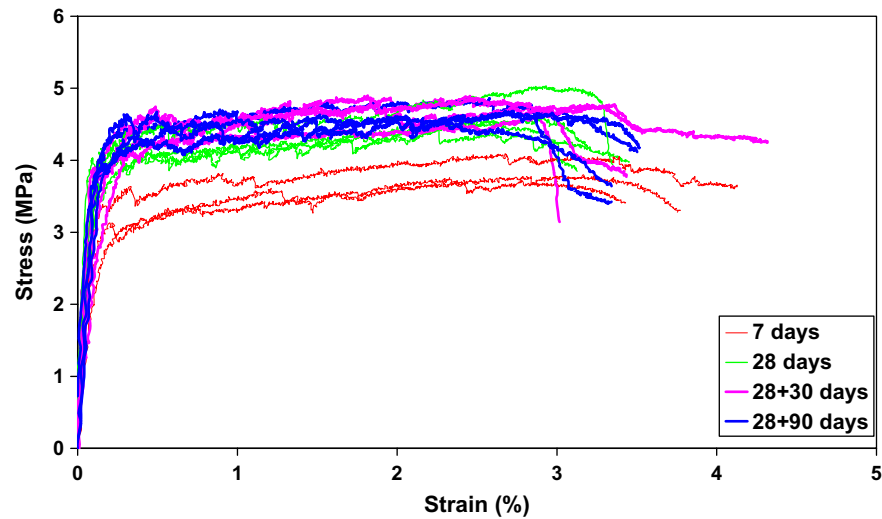


Fig. 4. Tensile behavior of ECC mixtures cured in air after 7 days moist curing.

Table 4
Tensile properties of ECC (M45) under alkali exposure conditions

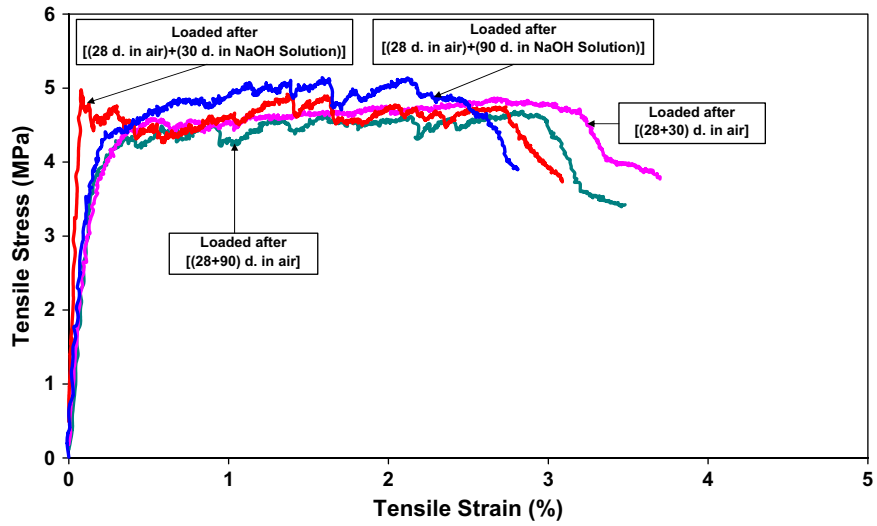
Specimen type	Tensile strain (%)	Tensile strength (MPa)	Residual crack width (μm)
<i>Specimens cured in laboratory air after 7 days moist curing</i>			
7 days	3.53 (0.18)	3.88 (0.24)	58.35 (23.48)
28 days	3.21 (0.12)	4.53 (0.27)	51.06 (17.80)
28 days + 30 days	3.13 (0.40)	4.75 (0.26)	44.01 (7.97)
28 days + 90 days	3.07 (0.26)	4.66 (0.14)	38.74 (12.50)
<i>Specimens stored in alkali solution at 38 °C</i>			
Uncracked, 30 days	2.80 (0.23)	4.64 (0.67)	86.18 (23.22)
Uncracked, 90 days	2.49 (0.56)	4.55 (0.17)	87.44 (37.59)
Pre-cracked-1.0%, 30 days	2.73 (0.37)	4.36 (0.19)	73.66 (18.43)
Pre-cracked-1.0%, 90 days	2.51 (0.21)	4.56 (0.46)	82.69 (36.9)
Pre-cracked-2.0%, 30 days	2.75 (0.41)	4.21 (0.13)	97.93 (35.63)
Pre-cracked-2.0%, 90 days	2.44 (0.38)	4.39 (0.45)	89.16 (53.38)

Numbers in parentheses are standard deviations.

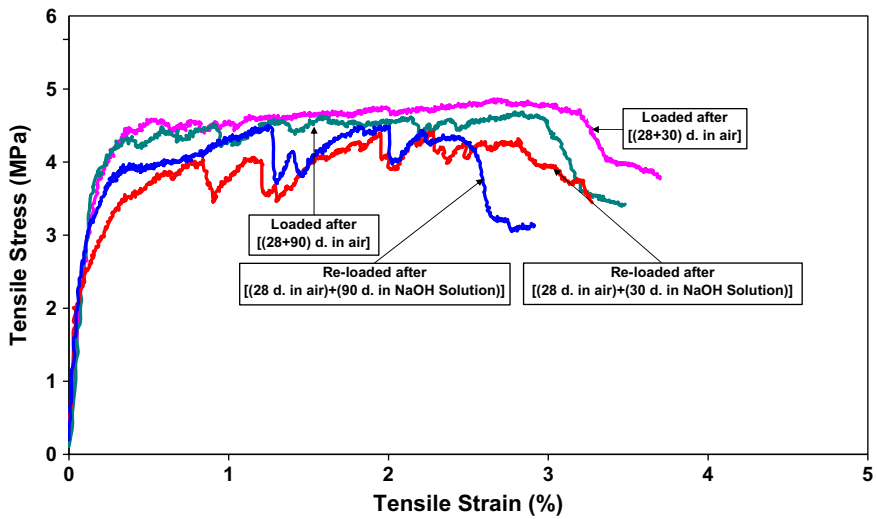
Table 4 also summarized the tensile strain capacity, tensile strength, and crack width of ECC with various pre-loaded strain values, and alkali exposure condition at 38 °C. Typical tensile stress–strain curves obtained for coupon specimens pre-cracked at 28 days and subsequently immersed in an alkali solution are shown in Fig. 5. Two sets of data are generated from specimens immersed for 30 and 90 days in alkali solution, and two pre-loading levels (1% and 2%) were employed. Typical stress–strain curves of control ECC specimen (cured in air) are also included in this figure. As seen in these figures, the first-cracking strength of pre-cracked ECC specimens after alkaline solution immersion falls below the first-cracking strength of the virgin specimens cured in air and in alkaline environment. Another distinct observation concerns the shape of the virgin and pre-cracked specimens. In the case of virgin specimens, the initial shape of the curves is almost linear up to about 90% of ultimate tensile load. The initial linear portion of the stress–strain curves of the pre-cracked specimens, however, extends only up to about 60% of the ultimate load. For the pre-cracked specimens, exposure

to alkali solution at 38 °C appears to exacerbate the deterioration. Moreover, a tendency of reduced tensile strength and tensile strain capacity with exposure age was noticed.

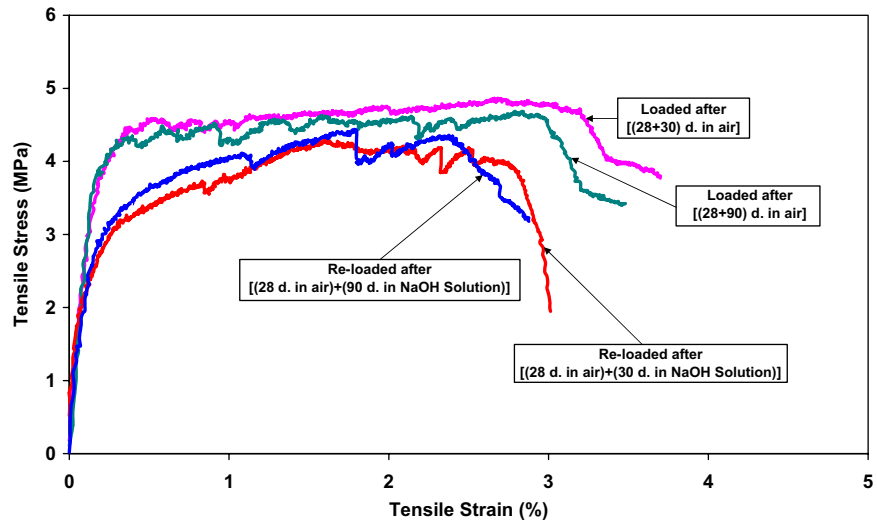
By comparing the initial material stiffness of reloaded ECC specimens stored in sodium hydroxide solution in Fig. 5 with that shown for the reloaded specimens before exposure in Fig. 2, it can be observed that a significant recovery of mechanical stiffness has been achieved. This suggests that between the time of inducing pre-cracking and the time of testing, after immersion in alkaline solution, healing of the micro-cracks has occurred in the ECC specimens. This can be attributed primarily to the high cementitious material content and relatively low water to cementitious material ratio within the ECC mixture. As a result of the formation of micro-cracks due to mechanical loading, unhydrated cementitious particles are easily exposed to the sodium hydroxide solution at 38 °C, which leads to development of further hydration processes. Finally, micro-cracks under conditions of a damp environment were closed by newly formed products. This observation is also supported by an environmental scanning



(a) Virgin (not pre-cracked) specimens



(b) Effects of pre-cracking to 1% tensile strain



(c) Effects of pre-cracking to 2% tensile strain

Fig. 5. Effect of alkali exposure on tensile behavior of ECC (M45).

electron microscope (ESEM) observation of the fractured surface of ECC across a healed crack. Fig. 6 shows that most of the products seen in the cracks were newly formed C–S–H gels. Calcium hydroxide (CH) and deposition of alkali salts in the crack path were also observed. These results indicate that micro-cracks of ECC exposed to sodium hydroxide solution healed even after exposure for 30 days to sodium hydroxide solution. In ECC, the re-healing process is especially aided by the innately tight crack width.

The average ultimate tensile strength values are summarized in Table 4. Compared to control specimens cured in laboratory air, the test results indicate that the ECC specimens stored in sodium hydroxide solution show a very slight reduction (especially for the pre-cracked specimens) in ultimate tensile strength for all exposure ages; this may be attributed to the effects of damage on the fiber/matrix interface due to immersion of humid/alkaline environment at 38 °C. However, more experimental studies on a micro-mechanical scale are necessary to understand the reasons of the reduction in the ultimate tensile strength.

Fig. 7 shows the average of tensile strain capacity of ECC specimens stored in sodium hydroxide solution. The tensile strain capacity summarized also in Table 4 for these specimens does not include the residual strain from the pre-cracking load. By neglecting this residual strain, the large variability in material relaxation during unloading is avoided, and a conservative estimation for ultimate strain capacity of the material is presented. The tensile strain capacity of virgin and pre-cracked ECC specimens exposed to sodium hydroxide solution averaged between 2.44% and 2.80%. The reduction in tensile strain capacity of ECC specimens stored in sodium hydroxide solution at 38 °C may be attributed to the effects of damage on the fiber/matrix interface. For example, Li et al. [7], examined the interfacial microstructure change of PVA-ECC in hot water (60 °C) exposure. They observed that after immers-

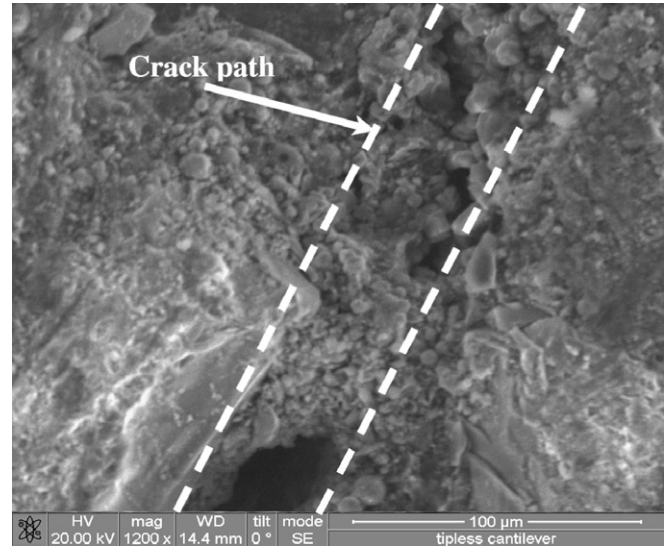


Fig. 6. ESEM micrograph of rehydration products in a self-healed crack after 30-day exposure period.

ing the composite in hot water for 26 weeks, the fiber bridging property has deteriorated through an increase in the chemical bond (G_d) of the fiber/matrix interface combined with a decrease in the apparent fiber strength (σ_{fu}^{APP}). This combination of changes in G_d and σ_{fu}^{APP} results in a $\sigma(\delta)$ curve that has small complementary energy J'_b (Fig. 1). Consequently, the condition for strain hardening as expressed in Eq. (1) is more readily violated in such composites after long-term exposure, leading to unsaturated multiple cracking and associated reduced strain capacity.

Despite a reduction in ductility, the ECC composites after 90 days of alkali solution exposure are found to retain tensile ductility more than 200 times that of normal concrete and normal fiber reinforced concrete with no environmental exposure. For this reason, it is expected that the ECC composites investigated are suitable for long-term

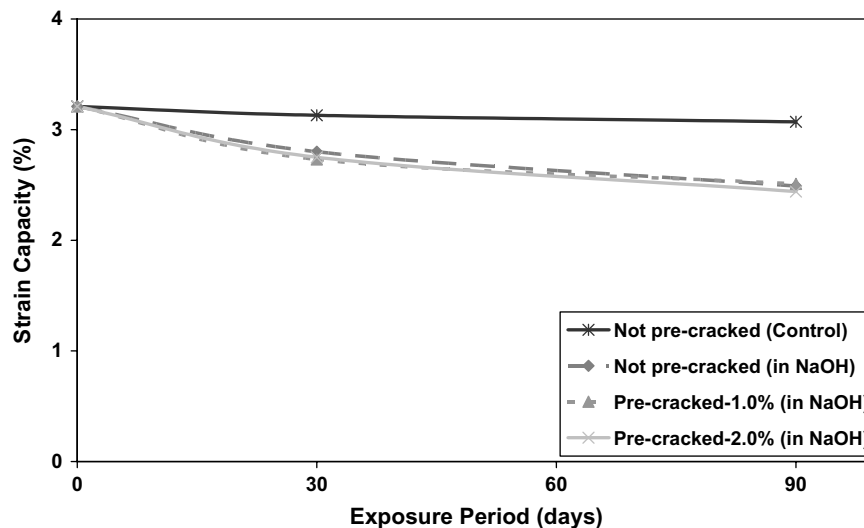


Fig. 7. Influence of sodium hydroxide solution at 38 °C and mechanical loading on ECC tensile strain capacity.

application under high alkaline environments if the structure is designed based on long term mechanical properties. Moreover, exposure condition used in this experimental study provides a continuous supply of alkali ions. Such a supply may not be available in real field conditions and therefore, the present test may impose a more accelerated and severe exposure environment when compared with real field conditions.

Table 4 also shows the residual crack width of ECC mixtures at different ages. The term residual crack width indicates that crack width was measured from the unloaded specimen after the uniaxial tensile test by using an optical microscope. Each average crack width in Table 4 was an average of those measured in four coupon specimens. The residual crack width of virgin and pre-cracked specimens exposed to sodium hydroxide solution is wider than that of virgin air cured specimens, but remains less than 100 μm . In terms of permeability and diffusion, crack width less than 100 μm generally behave like sound concrete [23,24]. Based on experimental results, Şahmaran et al. [24], Evardsen [25], Reinhardt and Jooss [26] proposed that cracks with width below 100 μm can be easily closed by a self-healing process. However, more experimental studies on a micro-mechanical scale are necessary to clearly understand the mechanisms behind the reduction in the ultimate tensile strength and increased crack width.

5. Conclusion

The results obtained from accelerated mortar bar test (ASTM C1260) indicated that ECC did not show any expansion at the end of 30 days soaking period probably due to non-reactive silica sand. However, even if reactive silica sand and alkalis are present in ECC, it cannot be expected to develop deleterious expansion due to alkali silica reaction because of the high volume fly ash content, small sand particle size and micro-fibers in ECC.

Pre-loaded ECC specimens with micro-cracks with width of about 50 μm induced by mechanical loading and then exposed to alkaline solution at 38 °C almost fully recovered their elastic stiffness when re-tested in direct tension. Moreover, self-healing of micro-cracks in ECC specimens subjected to sodium hydroxide solution is evident from the ESEM observations. On the other hand, alkali solution exposure at 38 °C leads to a reduction of about 20% in the tensile strain and about 4% in the tensile strength capacity of ECC at the end of the 90 days exposure period. Moreover, the crack width increased to around 100 μm compared with 40 μm in air curing condition. This phenomenon suggests possible change in the fiber/matrix interface bond properties. Apart from the slight reductions in ultimate tensile strain and tensile strength capacity and higher residual crack width, the results presented in this study largely confirm the durability performance of ECC material under high alkaline environment, even in cases where the material experiences mecha-

nical loading that deforms it into the strain-hardening stage prior to exposure.

The results presented in this study provide a preliminary database for the durability of cracked and uncracked ECC under combined mechanical loading and alkaline environmental loading conditions. For a complete understanding of durability of ECC in alkaline environment, it will be necessary to conduct further research on a micro-mechanical scale to investigate changes of ECC matrix toughness and fiber/matrix interface properties.

Acknowledgements

The first author would like to acknowledge the financial support of TUBITAK (The Scientific and Technical Research Council of Turkey). This research was partially funded through an NSF MUSES Biocomplexity Program Grant (CMS-0223971 and CMS-0329416). MUSES (Materials Use: Science, Engineering, and Society) supports projects that study the reduction of adverse human impact on the total interactive system of resource use, the design and synthesis of new materials with environmentally benign impacts on biocomplex systems, as well as the maximization of efficient use of materials throughout their life cycles.

References

- [1] Li VC. On engineered cementitious composites (ECC) – a review of the material and its applications. *J. Adv. Concrete Technol.* 2003;1(3):215–30.
- [2] Weimann MB, Li VC. Drying shrinkage and crack width of ECC. *Brittle Matrix Composites 7*, Warsaw, Poland; October 2003. p. 37–46.
- [3] Naaman AE. Tailored properties for structural performance. In: *Proceedings of the RILEM/ACI workshop: high-performance fiber-reinforced cement composites*. London (UK): E&FN Spon; 1992. p. 18–38.
- [4] Krstulovic ON, Malak S. Tensile behavior of slurry infiltrated mat concrete (SIMCON). *ACI Mater J* 1997;94(1):39–46.
- [5] Breitenbucher B. High-performance fiber concrete SIFCON for repairing environmental structures. In: *Proceedings of the third RILEM/ACI workshop: high-performance fiber reinforced cement composites*, London, UK; 1999. p. 585–94.
- [6] Li VC. Advances in strain-hardening cement based composites. In: *Engineering foundation conference on advances in cement & concrete*, New Hampshire; July 24–29, 1994.
- [7] Li VC, Horikoshi T, Ogawa A, Torigoe S, Saito T. Micromechanics-based durability study of Polyvinyl Alcohol-Engineered Cementitious Composite (PVA-ECC). *ACI Mater J* 2004;101(3):242–8.
- [8] Horikoshi T, Ogawa A, Saito T, Hoshiro H. Properties of Polyvinyl Alcohol Fiber as reinforcing materials for cementitious composites. In: *Proceedings of international RILEM workshop on HPFRCC in structural applications*, Published by RILEM SARL; 2005. p. 145–53.
- [9] Marshall DB, Cox BN. A *J*-integral method for calculating steady-state matrix cracking stresses in composites. *Mech Mater* 1988;8:127–33.
- [10] Li VC, Leung CKY. Theory of steady state and multiple cracking of random discontinuous fiber reinforced brittle matrix composites. *ASCE J Eng Mech* 1992;118(11):2246–64.
- [11] Lin Z, Kanda T, Li VC. On interface property characterization and performance of fiber reinforced cementitious composites. *J Concrete Sci Eng, RILEM* 1999;1:173–84.

- [12] Wang S, Li VC. Tailoring of pre-existing flaws in ECC matrix for saturated strain hardening. In: Proceedings of FRAMCOS-5, Vail, Colorado, USA; April 2004. p. 1005–12.
- [13] Li VC, Wu C, Wang S, Ogawa A, Saito T. Interface tailoring for strain-hardening PVA-ECC. *ACI Mater J* 2002;99(5):463–72.
- [14] Yang Y, Lepech MD, Li VC. Self-healing of ECC under cyclic wetting and drying. In: Proceedings of international workshop on durability of reinforced concrete under combined mechanical and climatic loads, Qingdao, China; 2005. p. 231–42.
- [15] Holt E. Contribution of mixture design to chemical and autogenous shrinkage of concrete at early age. *Cement Concrete Res* 2005;35(3):464–72.
- [16] Alasali MM, Malhotra VM. Role of concrete incorporating high volumes of fly ash in controlling expansion due to alkali-aggregate reaction. *ACI Mater J* 1991;88(2):159–63.
- [17] Thomas MDA, Shehata MH, Shashiprakash SG. The use of fly ash in concrete: classification by composition. *Cement Concrete Aggr* 1999;21(2):105–10.
- [18] Carrasquillo RL, Snow PG. Effect of fly ash on alkali-aggregate reaction in concrete. *ACI Mater J* 1987;84(4):299–305.
- [19] Park SB, Lee BC. Studies on expansion properties in mortar containing waste glass and fibers. *Cement Concrete Res* 2004;34(7):1145–52.
- [20] Haddad R, Smadi M. Role of fibres in controlling unrestrained expansion and arresting cracking in Portland cement concrete undergoing alkali-silica reaction. *Cement Concrete Res* 2004;34(1): 103–8.
- [21] Turanli L, Shomglin K, Ostertag CP, Monteiro PJM. Reduction in alkali-silica expansion due to steel microfibers. *Cement Concrete Res* 2001;31(5):825–7.
- [22] Lepech MD, Li VC. Long term durability performance of Engineered Cementitious Composites. *Int J Restor Build Monument* 2006;12(2):119–32.
- [23] Wang K, Jansen D, Shah S, Karr A. Permeability study of cracked concrete. *Cement Concrete Res* 1997;27(3):381–93.
- [24] Şahmaran M, Li M, Li VC. Transport properties of Engineered Cementitious Composites under chloride exposure. *ACI Mater J* 2007;104(6):303–10.
- [25] Evarnson C. Water permeability and autogenous healing of cracks in concrete. *ACI Mater J* 1999;96(4):448–54.
- [26] Reinhardt HW, Jooss M. Permeability and self-healing of cracked concrete as a function of temperature and crack width. *Cement Concrete Res* 2003;33(7):981–5.